Innovative Infrastructure Solutions (2023) 8:210
https://doi.org/10.1007/s41062-023-01179-6

TECHNICAL PAPER

# Potential of waste distorted bricks to produce internally cured concrete under adverse curing conditions

A. T. M. Masum[1] · M. R. Rahman[1] · M. A. Kafi[1] · S. Ghimire[1] · S. Akter[1] · T. Manzur[2]

Received: 31 January 2023 / Accepted: 30 June 2023 / Published online: 16 July 2023


## Abstract

In Bangladesh, every year around five billion distorted bricks are produced due to overheating. These distorted bricks are treated as wastes in brick fields and usually disposed under the soil causing significant negative environmental impact. Recent studies found that internally cured (IC) concrete, using saturated brick chips (BCs) as an internal curing medium partially in place of stone chips, experienced enhanced mechanical and durability properties than conventional concrete (NC) with stone aggregate when exposed to adverse curing conditions. Consequently, distorted brick chips (DBCs) appear to have considerable potential to produce IC concrete, provided that they possess adequate absorption and desorption capacities. Hence, an effort was made to explore the potential of DBC as internal curing agent when proper curing for concrete cannot be ensured. It was found that saturated DBC showed moderate absorption and satisfactory desorption property and could be used to produce IC concrete. IC samples with DBC experienced higher strength and enhanced resistance against chloride intrusion than their NC counterparts in the presence of improper curing. Moreover, significant economic and environmental benefit could be attained through the utilization of these waste distorted bricks partially in place of conventional stone chips.

**Keywords** Distorted brick waste · Desorption · Internal curing · Adverse curing condition · Corrosion initiation

## Introduction

Bricks are used as the primary material in majority of masonry constructions of Bangladesh. Moreover, brick aggregates are quite popular in the country as coarse aggregate in concrete production due to local scarcity of natural stone aggregates [1]. The conventional stone aggregates are relatively expensive in Bangladesh due to foreign import [2] and high demand, which are often not used in the construction of structural members requiring average strength and durability, particularly in rural areas and outskirts of cities. In such construction sites, locally manufactured brick aggregates are usually used as an alternative to stone chips, as coarse aggregate, to prepare concrete mixes due to their availability and low cost. In Bangladesh, bricks are generally produced by manual molding of locally available clay soils from paddy fields followed by burning in the kilns, which causes differences in material composition due to variation in soil composition [2]. According to Department of Environment (DOE), Bangladesh database, around 7873 coal fired kilns along with 6 natural gas fired kilns are under operation to produce 34 billion of bricks per annum in the country [3, 4]. Generally, five different brick-burning technologies are being used in brick kilns, such as Fixed-Chimney Kiln (FCK), Zigzag, Hybrid Hoffman (HHK), Vertical Shaft Brick Kiln (VSBK) and Tunnel Kiln [5]. Despite having interventions from DOE, comparatively less energy-efficient FCK and Zigzag technologies are still responsible for 92% of brick production in the country [5]. Commercially,

✉ T. Manzur
tanvirmanzur@ce.buet.ac.bd

A. T. M. Masum
masum@ce.mist.ac.bd

M. R. Rahman
ridwanurrahman56@gmail.com

M. A. Kafi
ashrafkafi73@gmail.com

S. Ghimire
sauravghimire96@gmail.com

S. Akter
sampa@ce.mist.ac.bd

[1] Department of Civil Engineering, Military Institute of Science and Technology, Dhaka, Bangladesh

[2] Department of Civil Engineering, Bangladesh University of Engineering and Technology, Dhaka, Bangladesh

four classes of bricks, namely picked or pick-Jhama (Type A), first class (Type B), second class (Type C), and third class (Type D), are produced in the brick fields. Nomenclature of these commercially produced bricks is done as per the descending order of burning concentration inside the kiln [2]. Brick field owners aim at producing mainly Type A and Type B bricks as they are being used in masonry works as well as coarse aggregate in reinforced concrete (RC) [2]. However, due to improper temperature control in the kiln, it is often difficult to control the quality of brick production. Moreover, according to previous studies [2] and the survey conducted in different brick fields of the country, it has been found that approximately 10–15% of bricks are being over-heated from a single burn inside the kiln due to uncontrolled heating process. These bricks are highly irregular in shape and size, darker in color, partly swollen and flattened (shown in Fig. 1), which undergo heavy distortion due to uneven shrinkage. Such distorted bricks (say Type E) are rejected by the brick producers as they cannot be used either in construction or masonry works. Hence, they are treated as wastes in brick fields. Disposal and management of these waste bricks have been a crucial concern to the brick producers as well as to the DOE. Generally, these waste bricks are disposed under soil in the vicinity of brick fields inviting extra man power and transportation. Such disposal method affects the nearby soil by reducing fertility in crop production and thus causes environment pollution. Besides, some of these distorted bricks (less distorted and overheated) are mixed with other types of bricks especially with Type C and Type D to minimize the loss incurred from the generation and disposal of these waste bricks.

In the context of Bangladesh, alternative use of distorted bricks is of immense importance for managing such large quantity of wastes. A potential application of distorted bricks could be in the production of concrete as internal curing agent where proper curing conditions are difficult to maintain. Recent studies conducted at Bangladesh University of Engineering and Technology (BUET) showed that brick chips (BC) produced from Type A and Type B bricks can absorb a large amount of water while mixing and are capable of desorbing it later under ideal conditions [6, 7]. Such impressive absorption and desorption properties of BC make it an efficient internal curing agent where curing of concrete is done by itself from inside of the concrete matrix [8, 9]. Those studies showed that internally cured (IC) concrete, with around 20% substitution of conventional stone chips (SC) by saturated BC, produced better concrete in the absence of proper curing conditions [6, 7]. Another study by the same research group showed that under unfavorable curing conditions, IC concrete produced from saturated BC as internal curing medium yielded lower chloride diffusion coefficient [1]. As such, time to corrosion initiation was delayed significantly in IC concrete [1]. The saturated BC, as internal curing agent, hinders the creation of voids inside the concrete due to improper curing by supplying additional internal water for hydration under adverse curing conditions. In light of the earlier studies, it seems that distorted brick chips (DBC) could also be used as an internal curing medium within concrete for supplying additional water during hydration if they possess adequate absorption and desorption capacities. It is likely that lower absorption capacity of DBC, owing to over-heating and distortion, would result in lower efficacy as an internal curing medium in comparison with commercially produced bricks of superior quality (Type A and Type B). Nevertheless, moderate degree of internal curing from DBC could contribute significantly in management of such huge quantities of waste bricks.

**Fig. 1** Distorted bricks in brick field

It is evident that appropriate curing is crucial to produce concrete with desired mechanical properties. However, ensuring appropriate curing requires strict quality control protocol, which is often difficult to achieve in construction sites, particularly at remote regions, due to ignorance of workers and improper supervision [6, 10–14]. Degradation in durability and strength due to improper curing is further aggravated in saline conditions affecting the service life of RC structures adversely [15, 16]. Therefore, internal curing can overcome the shortcomings of concrete under unfavorable curing conditions by ensuring enhanced saturation within the cement matrix during hydration. In this study, an effort was made to explore the potential of DBC to produce IC concrete with better mechanical and durability properties when subjected to improper curing. Initially, the water absorption and subsequent desorption capacities of DBC were measured to ascertain the water release capacity of DBC under various relative humidity (RH) values. The pore structures of DBC and first class (Type B) BC were observe and compared using scanning electron microscope (SEM) images. Concrete specimens were produced with 20% partial replacement of SC by saturated DBC as IC samples and without DBC (with stone chips only) as control samples. IC samples with 20% BC were also made for comparison. The

performance of the produced IC (with both DBC and BC) concrete was then assessed and compared with control samples in terms of strength (compressive strength as per ASTM C39 [17]) and permeability (chloride diffusion coefficient as per NT Build 492 [18]) under different simulated unfavorable curing conditions in the laboratory. Six different simulated improper curing conditions were considered ranging from severe to moderate adverse curing. Finally, the effect of inclusion of DBC, as internal curing agent within concrete, on chloride induced time to corrosion initiation (TCI) was predicted according to the FIB code [19]. Chloride-induced corrosion of RC structures primarily depends on the resistance of concrete against intrusion of chloride ion, which is usually evaluated by the chloride diffusion co-efficient from non-steady-state migration test [18, 20–23]. Improperly cured concrete is left with a lot of interconnected voids, due to loss of water by evaporation and inadequate hydration, which act as continuous medium for chloride ion to intrude easily [24, 25]. As a result, resistance of concrete against chloride intrusion is significantly decreased, which in turn makes the RC structures more susceptible to corrosion with reduced TCI [26–31]. Additional water supplied by internal curing agents can be expected to ensure relatively better hydration under such inadequate curing and consequently, delay TCI of a RC structure.

The main objective of the research work was to evaluate the potential of distorted brick chips (DBC) as internal curing (IC) medium in enhancing the strength and durability of RC structures against chloride-induced corrosion under adverse curing conditions. After a comprehensive literature review, it was found that there is lack of significant research on this issue focusing the use of waste bricks of brick fields in the construction sector. The authors believe that the outcomes of this study will not only contribute in the management of waste bricks by utilizing significant amount of the same in construction sectors but also compensate economic loss incurred by brick producers. However, further study will be required to get complete insight on application of DBC to produce IC concrete.

## Materials and mix design

### Materials collection

The over-burnt distorted bricks were collected from commercial brick fields located near Dhaka, the capital of Bangladesh. The distorted bricks were crushed to prepare DBC to be used as internal curing agent. Standard first class bricks (Type B) were also collected to prepare BC and compare the properties of BC to that of DBC. Besides, locally available conventional stone chips (SC) and 'Sylhet' sand were collected to use as coarse aggregate (CA) and fine aggregate

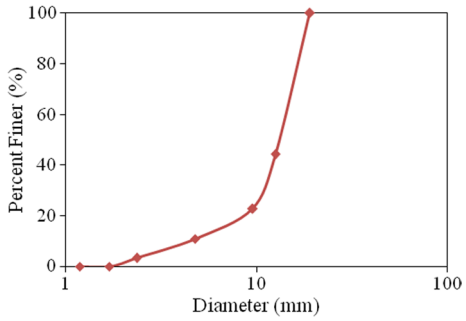


**Fig. 2** Gradation curve for CA

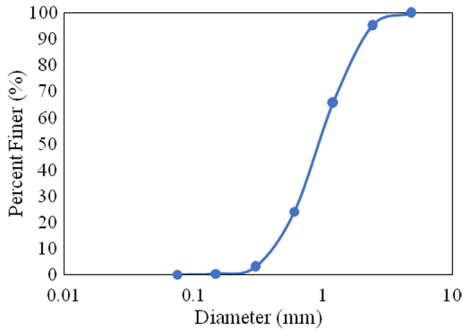


**Fig. 3** Gradation curves of FA

(FA), respectively. Ordinary Portland cement (OPC) (similar to ASTM Type 1) was used as binding materials. Sieve analysis of CA (SC) and FA (sand) was performed to get their gradation curves as per ASTM C136 [32]. The gradation curves of both CA and FA are shown in Figs. 2 and 3, respectively.

Fineness moduli (FM) values of CA and FA were obtained as 6.64 and 2.69, respectively. Bulk specific gravity (OD) of both SC and DBC was measured as per ASTM C127 [33] and found to be 2.71 and 1.70, respectively. Besides, absorption capacity of SC, BC, and DBC was determined to be 0.65%, 12%, and 8%, respectively. Similarly, bulk specific gravity and absorption capacity of sand were evaluated as 2.65 and 1.16%, respectively, as per ASTM C128 [34]. Moreover, unit weight of SC, BC, DBC and sand was determined as 1485, 995, 1010 and 1550 kg/m$^3$, respectively, following ASTM C29 [35] specifications. According to ASTM C187 [36] and ASTM C191 [37], the normal consistency and setting time of OPC were measured to be 27.2%, and 155 min (Initial) and 240 min (Final), respectively. On the other hand, its fineness was computed as 28.2 m$^2$/kg following ASTM C204 [38]. Subsequently, cement mortar's compressive strength was measured in accordance with ASTM C109 [39] and 28-day mortar strength was obtained as 32.80 MPa satisfying the code requirement [40].

## Mix design

Concrete mixes were prepared to attain a moderate strength in the range of 25 to 30 MPa, which is quite common in ordinary concreting works. After several trial, a mix ratio of 1: 2.1: 2.8 (cement: FA: CA) on weight basis with water-to-cement (w/c) ratio of 0.50 was selected that resulted in compressive strength of around 30 MPa for normal concrete or control sample kept under standard curing environment. Two types of concrete cylinders were produced following this ratio. One set of samples were produced with only SC as CA, which has been termed as control samples (NC). Another two sets were prepared with 20% replacement of SC by BC (Type B) and DBC as internal curing agent, which have been termed as internally cured (IC) samples: IC(B) and IC(E), respectively. All sets of concrete samples were kept under the laboratory-simulated curing conditions after casting. Besides, one set of sample was additionally prepared with only SC as CA with 28-day curing under water to represent standard normally cured concrete samples designated by NCS. The mix design was developed for such NCS sample to achieve target strength of around 30 MPa as mentioned above. Table 1 presents approximate amounts of constituents needed to prepare 1 $m^3$ of concrete for the weight-based mix ratio of 1: 2.1: 2.8. All the collected materials were converted to saturated-surface-dry (SSD) condition in the laboratory prior to mixing.

## Simulated adverse curing conditions

After casting, all NC and IC samples were subjected to 6 (six) adverse simulated curing conditions (ranging from severe to moderate) in the laboratory. Table 2 presents the descriptions and abbreviations of various simulated curing conditions. The severity of adverse curing conditions was expressed numerically from 1 to 6 where 1 represents the extreme adversity considered in the study. One set of IC(B), IC(E) and NC samples were kept outside the laboratory without any cover immediately after the casting to simulate the most severe curing conditions, which was designated as "1" in terms of the degree of severity. These samples were designated as IC(B/E)0W and NC0W, respectively (Table 2). Likewise, another set of both types of samples termed as IC(B/E)0P and NC0P, respectively, were exposed to similar conditions but with polythene covering. On the other hand, another two sets of IC samples and one set of NC samples were exposed to ambient condition after curing under water for 3 and 7 days to represent comparatively less severe curing conditions. Moreover, in order to simulate the ideal curing environment, one set of samples, termed as NCS prepared with SC as CA only was submerged under water for a period of 28 days. Figure 4 shows various simulated curing conditions in the laboratory.

# Experimental program and methodology

## Desorption test of brick aggregates

The desorption test of DBC was performed as per ASTM C1761 [41]. The desorption of BC was also conducted for comparison. Like any lightweight aggregate (LWA), the efficacy of DBC aggregate as internal curing agent can be evaluated by its absorption and desorption properties [42].

**Table 1** Approximate amounts of constituents needed for 1-$m^3$ concrete

| Water/cement ratio | Cement (kg) | FA (kg) | Percent replacement of SC by BC (%) | SC (kg) | BC (kg) | Slump (mm) |
|---|---|---|---|---|---|---|
| 0.50 | 353 | 736 | 0 | 1000 | 0 | 55 |
| | | | 20 | 800 | 200 | 61 (Type B) |
| | | | | | | 64 (Type E) |

**Table 2** Simulated curing conditions and their abbreviations in the laboratory

| SL | Simulated curing conditions | Degree of severity | IC(B)/IC(E) Samples | NC samples |
|---|---|---|---|---|
| 1 | Exposed just after casting without any cover | 1 | IC(B/E)0W | NC0W |
| 2 | Exposed just after casting and covered with polythene | 2 | IC(B/E)0P | NC0P |
| 3 | Exposed after 3 days of curing under water and without any cover | 3 | IC(B/E)3W | NC3W |
| 4 | Exposed after 3 days of curing under water and covered with polythene | 4 | IC(B/E)3P | NC3P |
| 5 | Exposed after 7 days of curing under water and without any cover | 5 | IC(B/E)7W | NC7W |
| 6 | Exposed after 7 days of curing under water and covered with polythene | 6 | IC(B/E)7P | NC7P |
| 7 | Curing under water for 28 days | – | NCS | |

**Fig. 4** **a** Standard curing condition (under water) and **b** adverse curing conditions with and without cover

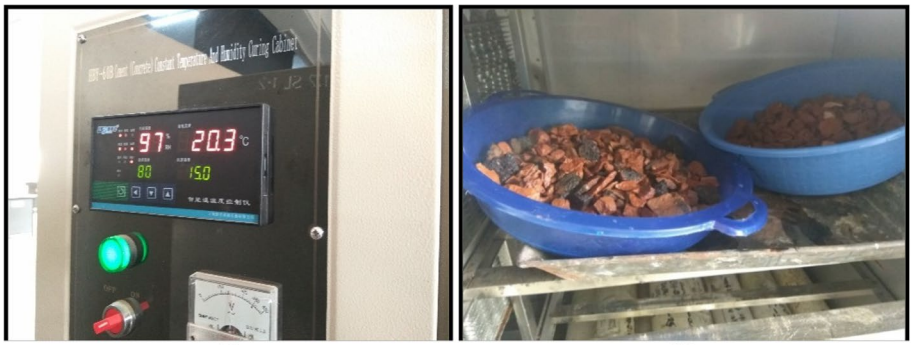

**Fig. 5** **a** Dehumidifier and **b** DBC samples inside the dehumidifier

Consequently, desorption test of the saturated DBC was conducted using a dehumidifier (Model: HBY-60B), as shown in Fig. 5a, to determine its efficiency in desorbing of absorbed water following ASTM C1761 [41]. A total of 20 different tests were performed in the humidifier having a wide range of temperatures and relative humidity (RH) values. Tests were performed for four RH values of 70, 80, 90, and 95% and five different temperatures of 15, 20, 25, 30, and 35 °C. In order to perform desorption test, DBC aggregates were made fully saturated by water under a vacuum chamber known as desiccator. After that, these DBC samples were put inside the dehumidifier at the aforementioned temperatures and RHs as shown in Fig. 5b. Loss of water was measured at 1-h interval by weighing until the measured weight becomes constant.

## Pore structure of BC and DBC

The microstructure of standard BC and over burnt DBC was investigated by scanning electron microscope (SEM) images. The SEM images were captured using Jeol JSM-7600F Schottky Field Emission Scanning Electron Microscopy (FE-SEM). The pore structure of BC and DBC was analyzed using SEM images and ImageJ software in order to complement the macro-behavior of aggregates through micro-structure. Smile View software was also used to evaluate tentative size of pores from the SEM images.

## Compressive strength test

The compressive strength tests of IC (made with both BC and DBC), NC and NCS samples were conducted following ASTM C39 [17] standard. The IC, NC and NCS samples (100 mm-by-200 mm concrete cylinder) were taken out from each simulated curing condition after 28 days for compressive strength test. The cylindrical samples were subjected to axial load by compression machine until failure at a rate of 0.15 MPa/s.

## Non-steady-state rapid migration test

To compute the chloride migration co-efficient, a non-steady-state migration test (RMT) was conducted for all IC, NC and NCS samples following NT Build 492 [18] standard. The chloride diffusion co-efficient of concrete samples was measured following Eq. (1) from the NT Build 492 [18].

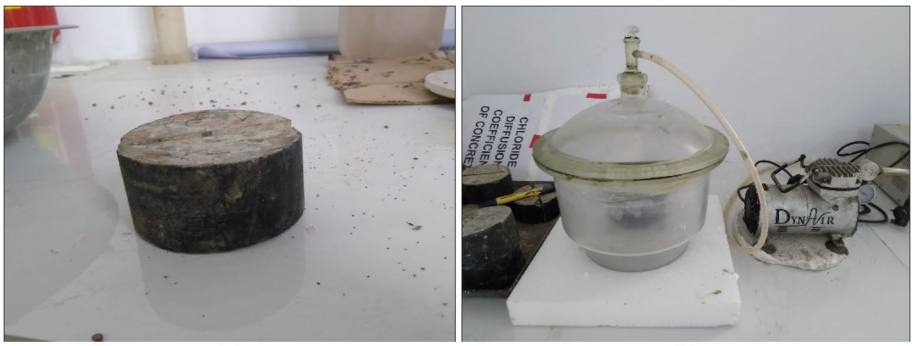


**Fig. 6** Sample preparation: **a** epoxy-coated test specimen and **b** preconditioning

The migration tests of all samples were carried out when the samples were of 45 days old. For the migration test, 50-mm-thick cylindrical samples were prepared from formerly cast cylinders. The specimen's surface was dried, and epoxy (Fig. 6a) coating was applied to side surface in order to restrict chloride intrusion only through the exposed end surfaces. When the epoxy was dried, the specimen was vacuum-saturated by using a desiccator (Fig. 6b) and submerging under $Ca(OH)_2$ solution for 20 h. The vacuum-saturated samples were submerged under 10% NaCl catholyte solution and 0.3 M NaOH anolyte solution in the migration test setup as shown in Fig. 7a [18]. Chloride ion from catholyte solution of NaCl was forced to penetrate the concrete samples by applying external power. The test was carried out for 24 h duration and at the end of the migration test; the specimen was divided axially into two halves. A spray of 0.1 M silver nitrate solution was applied on one of the freshly split sections (Fig. 7c) that reacted with the $Cl^-$ ion resulting silver

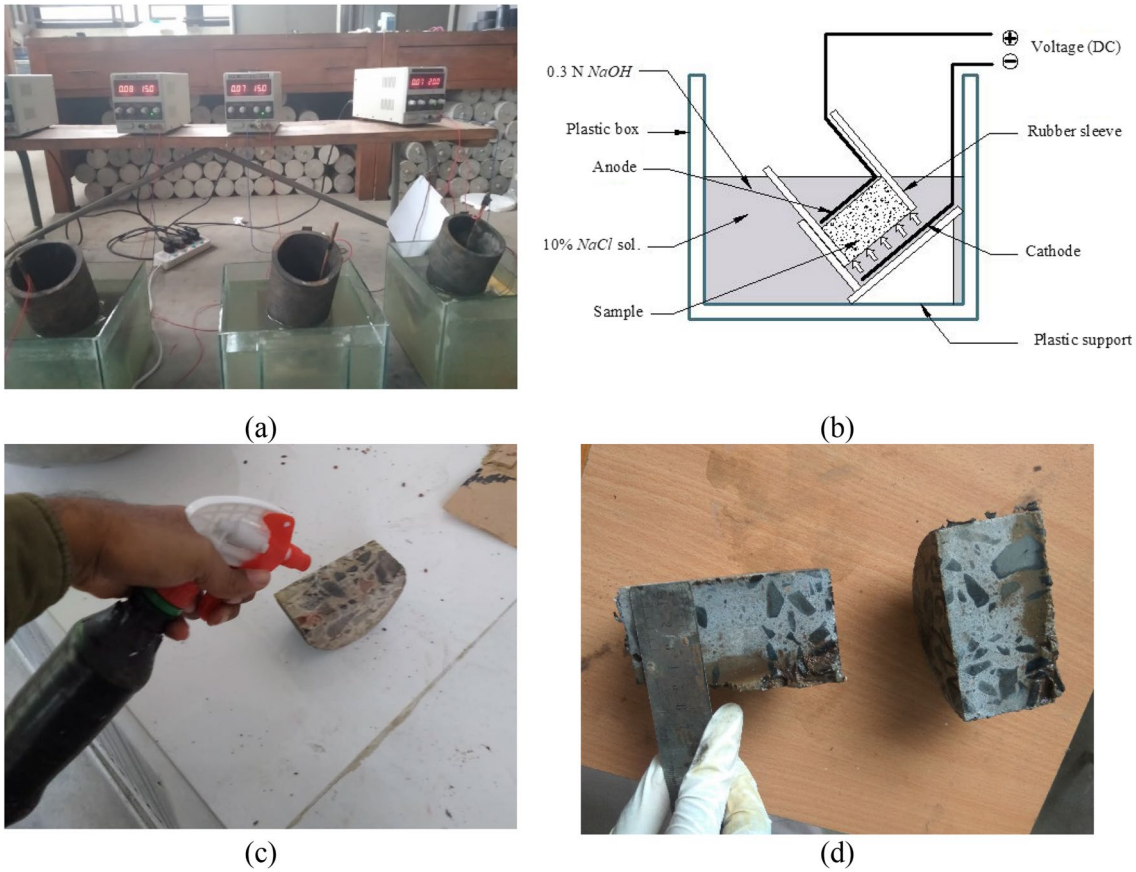


**Fig. 7** Non-steady-state migration test **a** experimental setup, **b** schematic view, **c** spraying of $AgNO_3$ on tested specimen and **d** chloride penetration depth measurement

chloride precipitation (white). Using a ruler, the depths of visible white silver chloride precipitation were measured at a 10-mm interval (Fig. 7d). Finally, chloride diffusion coefficient of different tested concrete samples was calculated from penetration depths of silver nitrate, applied voltage and temperature using Eq. (1) [18].

$$D_{\text{nssm}} = \frac{0.00239(273+T)L}{(U-2)t}\left(x_d - 0.0238\sqrt{\frac{(273+T)Lx_d}{U-2}}\right) \quad (1)$$

where

$D_{\text{nssm}}$: chloride migration coefficient, (in $10^{-12}$ $m^2/s$);

$U$: voltage applied (absolute value), V;

$T$: temperatures in the anolyte solution (average of initial and final), °C.

$L$: thickness of the sample, mm;$x_d$: depths of penetration (average), mm;$t$: duration of test, hour.

## Surface resistivity test

Surface resistivity test was conducted on all set of samples using a "Proseq Resipod" following AASHTO TP 95 code [43]. Surface resistivity (SR) measurement provides information about the likelihood of corrosion and the rate of corrosion of reinforced concrete. In order to conduct resistivity measurement, the concrete cylinder was first oven-dried and then vacuum-saturated with lime water. After that samples were submerged under water for duration of 18 h to measure saturated surface resistivity using the resipod. The tested concrete surface was brought in contact with the caps of outer probes by firmly pressing the resipod over it as shown in Fig. 8. The resistivity values of the tested mixes were displayed on the screen of the instrument. The measured resistivity values were then corrected applying geometric and temperature correction factors [44–46] as discussed in the following sections.


**Fig. 8** Surface resistivity measurement

### Factor for geometry effects

The Wenner probe was used for measurement of surface resistivity of the concrete samples. Since concrete surface resistivity provides information about the ability of concrete to resist chloride penetration, it is an important parameter to understand the durability of concrete. However, resistivity is independent of the geometry and configuration of the specimen [47]. Generally, commercially available devices like Proceq Resipod measure the concrete resistance. The measured resistance is then corrected for specimen geometry using a geometry factor ($k$), considering the specimen size, shape, and electrode configuration [47]. The corrected resistivity value ($r$) is determined by multiplying the geometry factor ($k$) with the resipod reading (R) as provided in Eq. 2.

$$r = R.k \quad (2)$$

Figure 9 schematically shows fundamental principle of surface resistivity measurement. It is required to use large spacing ($s$) of probe tip during resistivity measurement for avoiding aggregate interference that ensures infinite half-space achievement ($s \ll d$, $L$, where $d$ and $L$ are the diameter and length of cylinder, respectively) [48]. However, in cylindrical specimen,

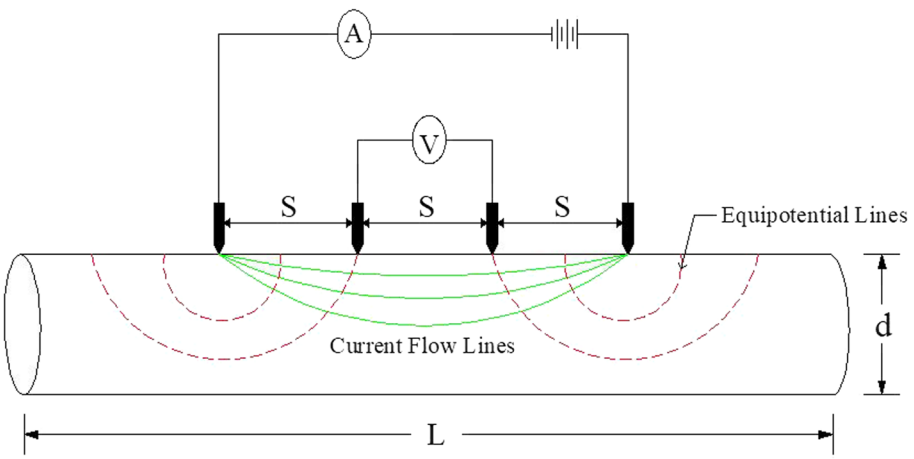


**Fig. 9** Surface resistivity measurement principle

the large spacing cannot be maintained due to smaller sample dimension, and hence, the geometry factor ($k$) of cylindrical specimen is measured through Eqs. 3–5. The Proceq Resipod [49] automatically applies adjustment for $k_1$ to the readings, and therefore, the value of $k_1$ should be taken as unity in Eq. 3.

$$k = \frac{k_1}{k_2} \tag{3}$$

$$k_1 = 2\pi s \tag{4}$$

$$k_2 = 1.10 - \frac{0.730}{\left(\frac{d}{s}\right)} + \frac{7.34}{\left(\frac{d}{s}\right)^2} \tag{5}$$

### Factor for temperature correction

Temperature also influences surface resistivity measurement of concrete samples, and therefore, correction for temperature is needed with respect to a reference temperature. Surface resistivity values are corrected for temperature using the activation energy-based relationship [47], as given in Eq. 6.

$$\frac{r_{T_{\text{ref}}}}{r} = \exp - \frac{E_{\text{a-cond}}}{R}\left(\frac{1}{T} - \frac{1}{T_{\text{ref}}}\right) \tag{6}$$

In Eq. 6, $r_{T\text{ref}}$ is the corrected resistivity, $r$ is the resistivity measured at temperature $T$, $E_{\text{a-cond}}$ is the activation energy, $R$ is the universal gas constant (8.314 J/k/mol) and $T_{\text{ref}}$ is the reference temperature (23 °C). In this study, surface resistivity was measured at temperature 25 °C. The activation energy for OPC mixes was taken as 25.1 kJ/mol from a previous study by Spragg [47].

## Prediction of service life

In the marine environment, durability of any RC structure is typically measured by its resistance against chloride-induced corrosion. Such resistance is described by the accumulation of critical chloride level on the rebar's surface to initiate corrosion through depassivation of the inherent protective layer due to the reduction in pH within concrete matrix and subsequent propagation of the cracks beyond allowable limit. As such, service life against chloride-induced corrosion for of RC structures comprises of time required to initiate corrosion, time required to initiate crack and time required for the propagation of crack beyond the allowable limit. However, the primary component that determines the service life of RC structure is time to corrosion initiation as other two components are comparatively smaller in duration. Time to corrosion initiation (TCI) is determined by the accumulation of critical amount of chloride ions on the rebar's surface from outside environment by penetrating the concrete cover. As per European standard EN 206-1[42], four chloride-induced corrosion phenomena have been categorized into four exposure classes depending on the surroundings of a structure. A description of four exposure classes according to EN 206-1 [42] with chosen concrete covers (for analysis in the study) is presented in Table 3. For each class of exposure, different feasible cover values were selected in this study for

**Table 3** Various classes of exposure in relation to chloride-induced corrosion [42]

| Classes | Sub-classes | Description of the environment | Chosen concrete cover (mm) |
|---|---|---|---|
| Corrosion induced by chlorides other than from sea water (XD) | XD1 | Concrete surfaces exposed to airborne chlorides | 25 |
| | | | 37.5 |
| | XD2 | Parts of bridges exposed to spray containing chlorides, pavements, car park slabs | 75 |
| | | | 100 |
| | | | 125 |
| | | | 150 |
| Corrosion induced by Chlorides from sea water (XS) | XS1 | Structure near to or on the coast exposed to airborne salt | 37.5 |
| | | | 50 |
| | XS2 | Part of marine structures with the tidal, the splash and spray zone | 75 |
| | | | 100 |
| | | | 125 |
| | | | 150 |

**Table 4** Values of different parameters of Eqs. 7 and 8 [19]

| Parameters | Definition | XD1 | XD2 | XS1 | XS2 |
|---|---|---|---|---|---|
| $C_{crit}$ | Critical chloride content [wt.-%/c] | 0.60 | 0.60 | 0.60 | 0.60 |
| $C_0$ | Initial chloride content of the concrete [wt.-%/c] | 0.10 | 0.10 | 0.10 | 0.10 |
| $C_{S,}\Delta x$ | Chloride content at a depth Δx and a certain point of time t [wt.-%/c] | 1 | 2 | 1.5 | 2 |
| $\Delta x$ | Depth of the convection zone [mm] | 0 | 10 | 0 | 10 |
| $D_{crm(to)}$ | Apparent coefficient of chloride diffusion through concrete [mm$^2$/years] | From RMT test as per NT Build 492 [18] | | | |
| $k_t$ | Transfer parameter | 1 | 1 | 1 | 1 |
| $a$ | Ageing exponent | 0.65 | 0.30 | 0.65 | 0.30 |
| $t_0$ | Reference point of time [years] | 0.1233 | 0.1233 | 0.1233 | 0.1233 |
| $b_e$ | Regression variable [K] | 4800 | 4800 | 4800 | 4800 |
| $T_{ref}$ | Reference temperature [K] | 301 | 301 | 301 | 301 |
| $T_{real}$ | Temperature of structural element or ambient air [K] | 301 | 301 | 301 | 301 |

predicting TCI to achieve service life of around 50 years or more. Chloride-induced TCI was measured using the revised equations of DuraCrete [50, 51] and is shown in Eqs. 7 and 8. Different parameters of the equations, chosen from FIB Bulletin 34 [19], are provided in Table 4.

$$C_{crit} = C(x = a, t) = C_O + \left(C_S, \Delta x - C_O\right).\left[1 - erf\left(\frac{x - \Delta x}{2.\sqrt{K_e K_t \left(\frac{t_o}{t}\right)^a D_{crm}(t_o).t}}\right)\right] \quad (7)$$

$$\text{where } k_e = \exp\left(b_e\left(\frac{1}{T_{erf}} - \frac{1}{T_{real}}\right)\right) \quad (8)$$

## Results and discussion

After performing relevant tests pertaining to the study, obtained results are presented and discussed in depth. In this regard, appropriate graphs and bar charts are used to comprehend the relationship among them. Initially the results obtained from desorption test of brick aggregates are presented and discussed. Afterwards how internal curing affects concrete's compressive strength, chloride diffusion coefficient, surface resistivity and time to corrosion initiation under various adverse curing conditions simulated in the laboratory are discussed.

### Effect of temperature and RH on desorption rate of BC and DBC

Desorption rates in terms of absorbed water of BC and DBC for four different RHs and five different temperatures are presented in Fig. 10a and b, respectively. Earlier, the absorption

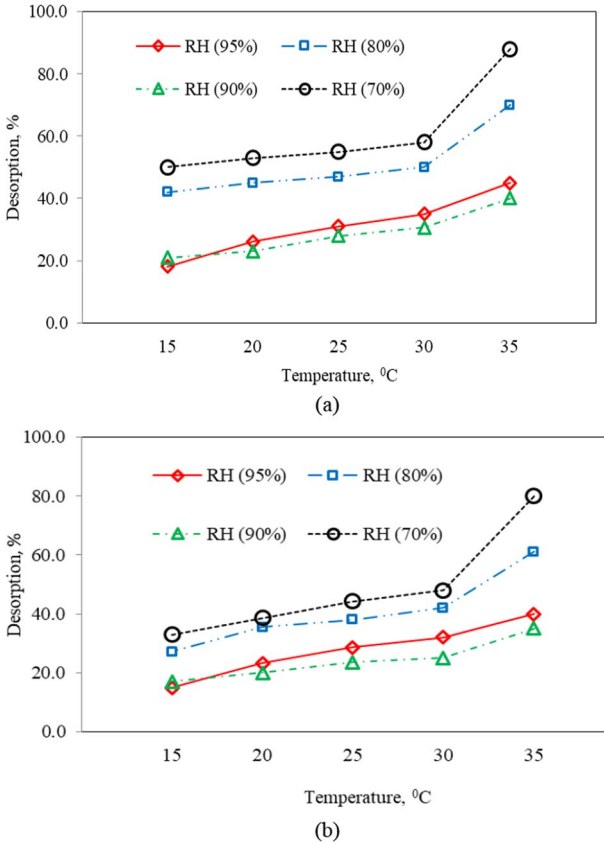


**Fig. 10** Effect of temperature and RH on desorption rate of **a** BC and **b** DBC

capacities of BC and DBC were found to be 12% and 8%, respectively. It was observed from desorption test that, in general, with the increase of temperature the desorption rate increased. On the other hand, reverse relationship was observed between relative humidity and desorption rate for both BC and DBC. It was evident from desorption test that maximum desorption rate of 88% and 80% was obtained

at RH of 70% (the lowest RH during experiment) and temperature of 35 °C (the highest temperature considered in the study) for BC and DBC, respectively. Such trend in desorption capacity was analogous to the previous findings on BC as internal curing medium within concrete [6, 7, 10]. Moreover, based on current desorption test results and previous studies [6, 7, 10], it can be inferred that DBC would experience desorption rate of more than 80% under reduced RH than that of 70%. On the other hand, minimum desorption rates of 18% and 15% for BC and DBC, respectively, were found at RH ranged between 90 and 95% and temperature of $15^0$C. It was also observed that the desorption rate become somewhat similar when the RH reached 90% and above. It was evident that DBC showed relatively lesser absorption and desorption capacity as compared to BC due its modified pore structure resulting from over-burning. However, even at higher RH of 95%, DBC showed desorption rate of around 40% of its absorbed water at relatively higher temperature, which confirmed the presence of extra water inside concrete matrix just after the casting when both RH and temperature remain considerably higher.

## Pore structure analysis of BC and DBC through SEM images

In this section, an attempt has been made to analyze the pore structure of BC and DBC using SEM images. ImageJ and Smile View software were used to have a general idea on size and area of pores within BC and DBC. In Fig. 11, the tentative size of pores measured through Smile View is shown. Figure 12 shows the SEM images of both BC and DBC with pores in the ImageJ environment. The images on left side show the pores on SEM images, and the outlines of the pores are shown in the images on right side of Fig. 12.

Visible pores in SEM images of BC and DBC were analyzed using both Smart View and ImageJ software to compare the size and distribution of pores within normal and over burnt brick matrix. It is evident from Fig. 11 that DBC had relatively larger pores as compared to its BC counterpart. Pores outlined by ImageJ software, as shown in Fig. 12, also matched with the observation from Smart View outcomes. The ImageJ software also provides quantitative numerical analysis of pores in terms of size [52]. The average size of pores of DBC was obtained as 104.6 $\mu m^2$, which is significantly higher than that of BC (34.9 $\mu m^2$). Feret's diameter is the measure of the longest distance between any two points along the selection boundary. Therefore, it is used to present the largest dimension of the pores from ImageJ analysis. Pores in DBC showed maximum Feret's diameter of 14.3 µm, whereas in case of BC, maximum Feret's diameter was obtained as 11.2 µm. The percentage area of pores in DBC was also higher as compared to BC. Numerically, 2.1% of area was occupied by the pores in DBC and 1.3% in case of BC. Therefore, it is obvious from SEM image analysis that DBC had larger pores than that of BC which matched with previous studies [53, 54]. Cultrone et al. [53] observed that over-burning of bricks resulted in increase in proportion of large pores and reduction of pore connectivity. The reduced absorption capacity of DBC as compared to BC, as discussed in "Materials collection" section, was due to such discontinuity between pores caused by over burning.

## Effect of IC on compressive strength

In Fig. 13, compressive strengths of all IC(B) and IC(E) samples are graphically presented using bar diagrams alongside NC samples for all simulated adverse curing conditions to show the variation among them. The

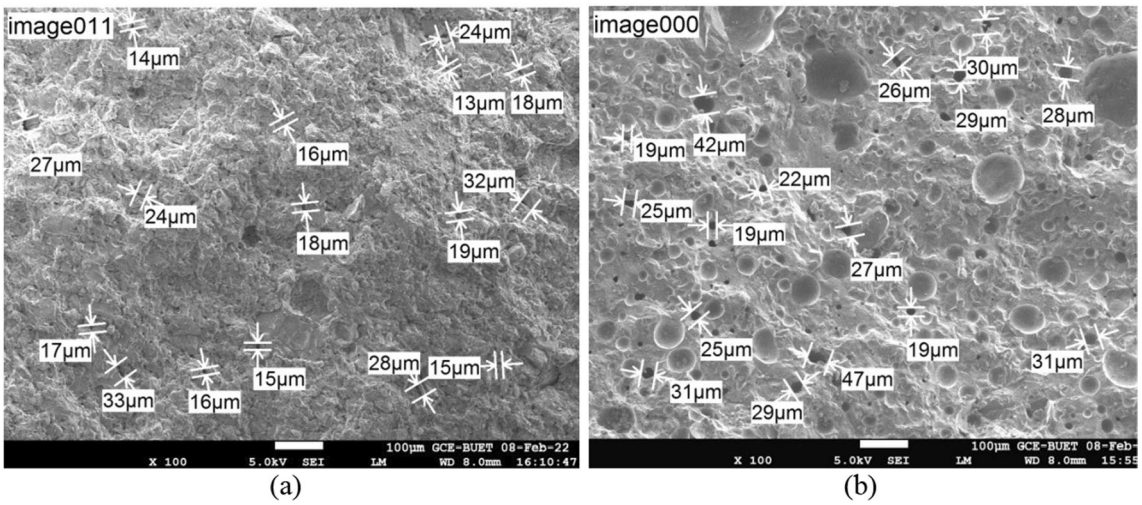


**Fig. 11** Tentative pore size using SEM images by Smart View of **a** BC, **b** DBC

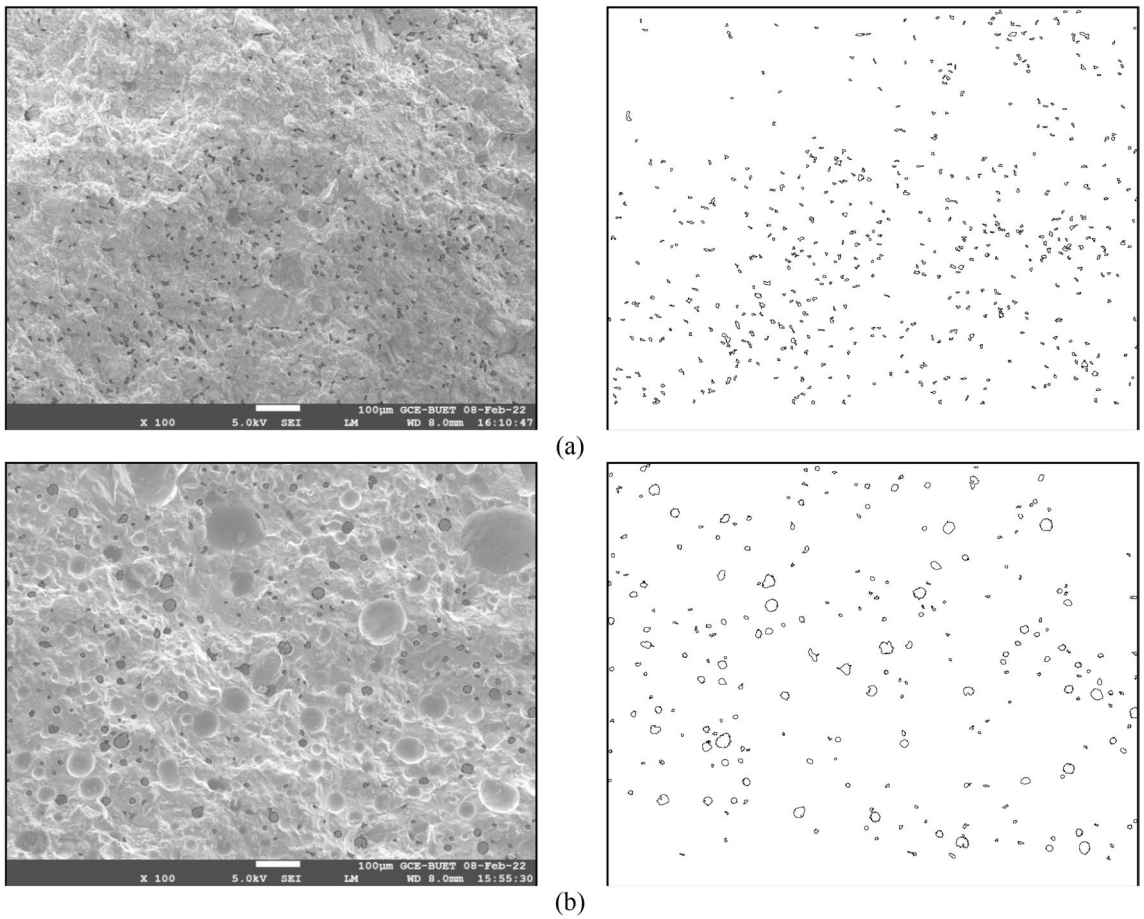


**Fig. 12** Analysis of pore structure using SEM images by ImageJ of **a** BC, **b** DBC

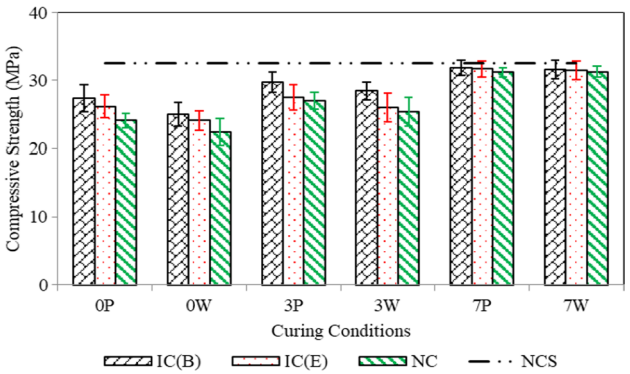


**Fig. 13** Effect of IC on compressive strength

compressive strength values provided in Fig. 13 are the mean of minimum three test results of each sample type. The error bars represent the standard deviation of measured compressive strength values of each sample. For comparison, dashed lines are used to depict the compressive strengths of control sample under standard curing (NCS). Trends in compressive strength results indicated 1–8% higher compressive strength for IC(E) samples than those of the corresponding NC sample under similar adverse curing condition. Particularly, under 0P and 0W curing conditions, which were comparatively harsher (Table 2), IC(E) sample showed 8% and 7% higher strength, respectively, than that of their NC counterparts. This clearly shows the efficacy of internal curing by DBC in terms of compressive strength of the resultant concrete. It was also found that IC(B) samples exhibited greater compressive strength as compared to their IC(E) counterparts due to relatively higher absorption and desorption ability of BC. For instance, under 0P and 0W curing conditions, IC(B) samples produced about 4.5% and 4% more strength than the corresponding IC(E) samples. However, under 7W and 7P condition, there is no significant difference between compressive strengths of concrete samples with or without IC. In fact, all samples showed almost similar strength when they were cured under water for 7 days and then covered with polythene sheets. Under such conditions, the NC samples gained considerable strength due to longer duration of submergence under water and consequent less evaporation. It should also be noted that sample with

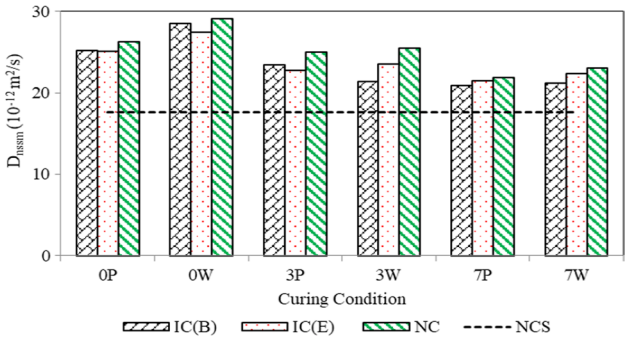


**Fig. 14** Effect of IC on chloride diffusion coefficients

polythene covering showed higher compressive strength than samples without any cover for all curing conditions. The IC(B) samples exhibited the highest compressive strength irrespective of adverse curing condition due to the higher absorption and desorption capacity of Type B brick as mentioned earlier. Under all simulated adverse curing conditions, concrete samples prepared from stone chips only (NC) exhibited lower compressive strength than that of IC samples due to the poor hydration, resulting from the loss of water by evaporation. On the other hand, the saturated brick chips acting as internal curing agent ensures better hydration in concrete by supplying additional water under such circumstances. Nevertheless, control samples (NCS) under ideal curing conditions produced the maximum compressive strength among all other samples.

## Effect of IC on chloride diffusion coefficients

In Fig. 14, chloride diffusion coefficients obtained from migration test are portrayed graphically for each IC and NC samples side by side for all adverse curing conditions. The bar diagrams represent average of at least three samples tested as per NT Build 492 [18]. Besides, diffusion coefficient of control sample (NCS) is also presented using dotted lines for better representation of comparison among them.

As seen from Fig. 14, IC samples (both B and E) showed lower chloride diffusion coefficients than their NC counterparts for all simulated adverse curing conditions. Numerically, about 2–9% lower migration coefficients were observed for the samples with IC(E) than corresponding NC one cured under the similar simulated conditions. This clearly indicates the superior performance of IC(E) samples (ensured by internal curing ability of DBC) over NC in terms of resisting chloride intrusion when exposed to adverse curing conditions. Besides, NC sample under 0W condition, which is considered as the most unfavorable curing condition of the study (Table 2), showed highest diffusion rate which was about 65% higher than that of properly cured NCS. Again, when compared to NCS samples, IC(E) samples under the same adverse curing condition (0W) experienced about 55% higher diffusion coefficient. Such behavior of IC samples is the effect of curing ability of DBC internally, which resulted in better hydration inside concrete. Similar to compressive strength results, DBC, as an internal curing agent, exhibited significant positive impact on the resistance of chloride intrusion under adverse curing environment. Moreover, it was observed that polythene covering exhibited better chloride resistance performance as compared to without covering condition due to prevention of loss of water through evaporation except in case of 3P and 3W curing conditions for IC(B) samples. Such inconsistency was probably due to variation in sample preparation and test conditions. It should also be noted that more prominent effect of covering was observed for "0" curing conditions since in this condition, samples were exposed just after casting.

## Effect of IC on surface resistivity of concrete

Resistivity determines the capability of concrete to resist the passage of electric ions into the concrete. Corrosive ions can easily pass through the concrete with high porosity and interconnected pore network. In Fig. 15, the variations in resistivity of the samples for various simulated curing conditions are shown. The dotted line in Fig. 15 represents surface resistivity of NCS sample.

Figure 15 shows that when compared under similar curing condition, IC samples exhibited reasonably higher surface resistivity than the corresponding NC ones. For instance, under 0P, 0W, and 3P conditions, IC(E) samples showed, respectively, 25%, 20% and 15% higher resistivity than corresponding NC samples indicating their superior resistance against chloride penetration. On the other hand, relatively less significant variations in surface resistivity were observed for samples cured under comparatively less critical curing conditions (like 7W and 7P). It was also found that, in general, concrete samples with IC(B) exhibited higher resistivity than that of their IC(E) counterparts due to better absorption and desorption ability of Class B aggregates.

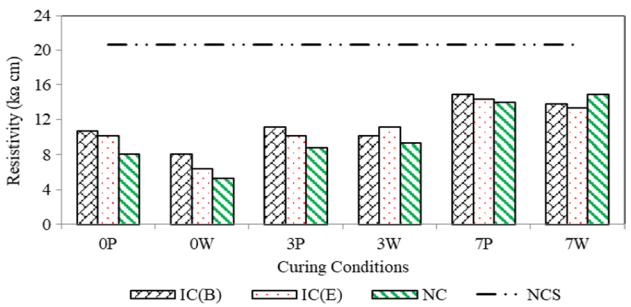


**Fig. 15** Effect of IC on surface resistivity of concrete

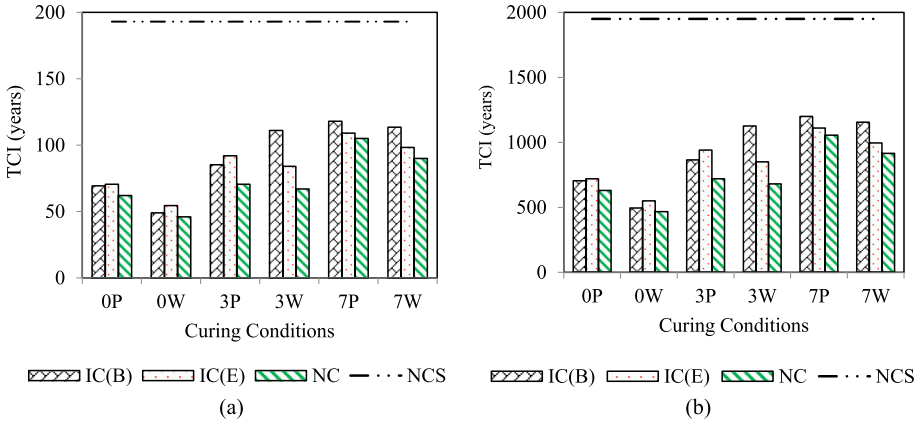


**Fig. 16** Effect of IC on TCI for XD1 and cover **a** 25 mm; **b** 37.5 mm

## Effect of DBC as internal curing agent on time to corrosion initiation (TCI)

The estimated corrosion initiation time (as per fib code) of all concrete samples under each adverse curing condition is presented in Fig. 16 through Fig. 18 for exposure category of XD1, XS1 and XD2/XS2, respectively. Such estimation of TCI is important to quantitatively evaluate the impact of internal curing on chloride-induced corrosion-related service life of RC element under adverse curing conditions. Moreover, results of concrete samples produced from IC (B and E) and NC are presented by bar diagram side by side in order to understand the effectiveness of DBC as internal curing agent. In addition, time to corrosion initiation of NCS is also displayed for comparison by dashed line.

In Fig. 16a, b, results of TCI for XD1 exposure are presented for concrete cover of 25 mm and 37.5 mm, respectively. In general, when cured under similar conditions, IC(B) samples experienced similar or slightly higher TCI than that of IC(E) samples due to their reduced migration coefficient, resulting from better absorption and desorption capacity of first class brick. It is also observed from Fig. 16a that when subjected to similar curing environment for concrete cover of 25 mm, both IC(E) and IC(B) samples showed higher corrosion initiation time in comparison with control sample. In case of relatively severe curing conditions, i.e., 0W, 0P, 3W and 3P, IC(E) samples exhibited reasonably higher time to corrosion initiation than their NC counterparts. On the other hand, under 7W and 7P curing conditions, the differences between TCI of internally cured samples and control samples were comparatively less. Similar trend was also observed for 37.5 mm cover from Fig. 16b where it showed significantly increased TCI for all internally cured samples considered in the study. Such behavior was the indication of the fact that DBC could be an effective IC agent under comparatively severe curing condition and XD1 exposure. However, TCI was considerably higher for 37.5-mm cover in comparison with 25-mm cover for all samples. For 37.5 mm-cover, all concrete samples regardless of curing conditions exhibited TCI of significantly higher than 100 years and therefore might not create durability issues regarding chloride-induced corrosion. However, for lesser cover, internal curing appears to provide reasonable increase in chloride-induced corrosion initiation time and

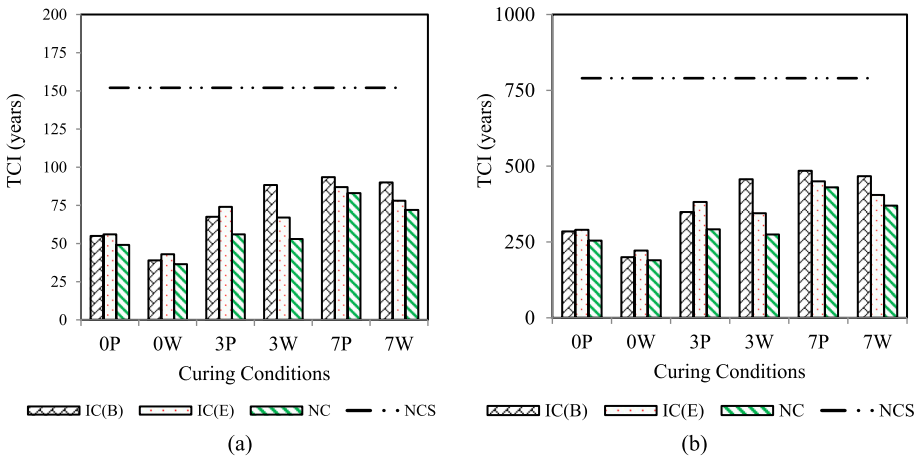


**Fig. 17** Effect of IC on TCI for XS1 and cover **a** 37.5 mm; **b** 50 mm

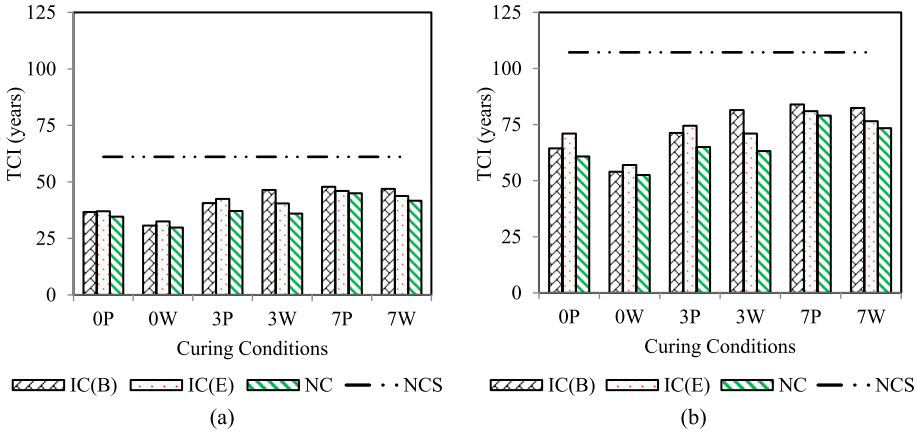


**Fig. 18** Effect of IC on TCI for XD2/XS2 and cover **a** 125 mm; **b** 150 mm

consequent enhancement of durability. Similar trend of significant delaying in corrosion initiation due to internal curing was observed for relatively lower cover values under other exposure conditions that have been discussed in the following sections.

The TCI values of IC and NC samples under XS1 exposure and with cover of 37.5 mm and 50 mm are shown in Fig. 17a and b, respectively. When subjected to similar curing conditions, IC samples experienced enhanced service life compared to NC samples echoing the pattern of previous exposure class. For 50-mm cover, all samples exhibited considerably higher TCI since XS1 exposure is reasonably less severe as compared to XD2 and XS2 exposure classes. In case of 37.5-mm cover, the delay in TCI for IC(E) samples ranged from 7 to 15 years for relatively severe curing conditions, i.e., 0W, 0P, 3W and 3P. Such delay in TCI was significant as compared to NC samples under these adverse curing conditions that ranged between 35 and 55 years. Therefore, benefit of using DBC as internal curing agent was apparent from the delayed TCI as compared to corresponding normal concrete under unfavorable curing environment.

Figure 18a, b illustrates the chloride-induced corrosion initiation time of all samples tested in the study under XD2/XS2 exposure class for concrete covers of 125 mm and 150 mm, respectively. The lower cover values than 125 mm, i.e., 75 mm and 100 mm, were not included since these cover values resulted in significantly reduced TCI (lesser than 25 years) for all IC and NC samples. This is due to the fact that XD2 and XS2 exposure classes represent the harshest exposure at which lower cover values appear to have less practical significance. Under these two exposure classes, the RC structures are directly exposed to spray containing chlorides or tidal and splash zones of marine environment. It is evident from Fig. 18a, b that all adversely cured IC samples showed delay in TCI as compared to NC samples. For instance, concrete sample with 150-mm cover and having comparative harsh curing environment of 0P and 0W showed about 4.5 and 10 years increment in TCI values in comparison with NC samples. On the other hand, under 3P and 3W conditions, IC(E) samples showed around 7.5–9.5 years delay in corrosion initiation for 150-mm cover. Such delay in TCI clearly indicates the efficacy of DBC to be used as IC agent for the RC structures, which are in direct contact with saline environment under adverse curing conditions.

## Economic benefit of using DBC as internal curing agent

Utilization of DBC as an effective construction material could have considerable impact on the economy of brick industry as well as construction sector of the country. Different aspects of economic benefit of DBC in relation to construction sector are summarized in Table 5. According to DOE database, annual production of useable bricks (commercial bricks) in the country is about 34 billion [3, 4]. In actual fact, total production of brick is around 38–40 billion as 10–15% got wasted due to uneven heating process in the kiln. This means annually around 5 billion (considering a

**Table 5** Snapshot of economic benefit of distorted brick chips

| Parameter | Unit | Quantity | Monetary value (BDT)[a] |
|---|---|---|---|
| Annual brick production (commercial) | Number | 34.0 billion [3, 4] | 333 billion (3.90 billion USD) [55] |
| Distorted brick generation (12.5%) | Number | 5 billion | 49 billion (5.55 million USD) |
| 20% Stone chips in $1m^3$ concrete (1: 2.1: 2.8) | $m^3$ | 0.13 | 825 (10 USD) [55] |

[a]1 USD = 82.5 BDT

mean wastage of 12.5%) waste bricks are being produced in the country.

It is evident from Table 5 that brick sector incurs around BDT 49 billion (USD 5.55 million) annually due to the unwanted generation of distorted bricks [55]. Moreover, these bricks are disposed under soil, which needs vehicle and manpower requiring more money for disposal. Besides, disposal of bricks under the soil can have significant negative impact on nearby soil and environment. On the other hand, price of stone chips is considerably high in the country as it has to be imported. So, replacement of 20% stone chips by DBC as coarse aggregate can significantly reduce the use of stone chips, which in turn reduce the cost of construction materials. Numerically, around 0.13 $m^3$ stone can be saved (considering mass based mix ratio of 1:2.1:2.8) per cubic meter of concrete reducing the cost of coarse aggregate around BDT 825 (USD 10) per cubic meter of concrete [55]. It is evident from the study that such replacement can be done in construction sites where proper curing is difficult to maintain. The IC concrete with 20% DBC exhibited TCI of significantly higher than 100 years for concrete cover of 37.5 mm and 50 mm under XD1 and XS1 exposure classes, respectively. Therefore, concrete with 20% DBC as partial replacement of stone aggregate can also be used when exposure class is less severe. Moreover, the compressive strengths of concrete with 20% DBC under 7P and 7W curing conditions were found to be comparable with the strength of control concrete exposed to ideal curing. The control concrete of the study was developed for moderate strength of 30 MPa as it is commonly used in ordinary construction works of the country. Therefore, concrete with 20% DBC appears to achieve equivalent strength of standard concrete with conventional stone aggregate for moderate strength range and under proper curing conditions. However, further studies will be required with larger sample sizes and mix variations to propose comprehensive guidelines in this matter. Nevertheless, the outcome of the study sheds light on the potential of utilizing waste distorted bricks in different types of construction scenarios of the country.

## Conclusion

This research was primarily conducted to investigate the potential of distorted brick chips (DBC) as internal curing agent to produce internally cured (IC) concrete with enhanced mechanical and durability performance as compared to control concrete under adverse curing conditions. Utilization of such waste distorted bricks as partial replacement of stone aggregates can also reduce economic loss, environmental pollution and usage of natural resources like stones. The outcomes of the study can be concluded as follows:

- Like any light weight aggregate (LWA), saturated distorted brick chips (DBC) possess moderate absorption and satisfactory desorption property to be used as internal curing agent within concrete. As the temperature rises and relative humidity (RH) drops, the rate of desorption of saturated DBC increases and vice versa. However, DBC experienced lesser absorption and desorption capacity than that of first class brick (Type B) chips (BC).
- It was found that IC samples with DBC as internal curing agent, i.e., IC(E) samples, showed 1–8% more compressive strength compared to NC sample under different simulated curing conditions of the study. The difference in strength between IC and NC samples was observed to be dependent on severity of the curing conditions. Under comparatively harsh curing environment (like 0P and 0W), relatively higher strength was obtained by IC(E) samples as compared to NC ones. Moreover, samples with polythene covering showed enhanced strength as compared to the samples without any cover for all considered curing environment.
- Under relatively less harsh curing phenomena (like 7P and 7W), concrete samples with DBC, i.e., IC(E) samples, exhibited comparable strength of normal concrete exposed to proper curing (NCS samples).
- Saturated DBC used as IC agent showed significant positive impact on the resistance to chloride intrusion, thus enhancing the durability issues of concrete. It was found that for different adverse curing conditions considered in the study, IC(E) samples showed 2–9% lower chloride diffusion coefficients than their NC counterparts when subjected to unfavorable curing conditions.
- The enhanced durability performance of IC samples was also validated through surface resistivity tests. Under relatively severe curing conditions, i.e., 0P, 0W, 3P and 3W conditions, IC(E) samples showed, on an average, about 20% higher resistivity than corresponding NC samples.
- Due to reduced chloride diffusion coefficient, higher corrosion initiation time was exhibited by IC(E) samples as compared to NC samples under similar simulated adverse curing conditions. Various exposure classes and concrete covers were considered in measuring time to corrosion initiation (TCI) of all the sets of samples considered. Under relatively less severe exposure classes like XD1 and XS1, IC(E) samples with typical cover of 37.5 mm or 50 mm exhibited satisfactory TCI for all the simulated curing conditions of the study. It was also observed that internal curing could provide reasonable delay in initiation of chloride-induced corrosion and consequent enhancement of durability when subjected to extreme exposure class, i.e., XD2 and XS2 under harsher curing conditions.
- About 5 billion bricks are being wasted annually in the country due to overheating in the kiln. The distorted

brick chips (DBCs) in the study were produced from such overheated brick wastes. Therefore, utilization of DBC as construction materials can have significant economic benefit. It was found from the study that DBC has considerable potential to be used as internal curing agent in construction sites where adverse curing conditions exist. Moreover, concrete with 20% replacement of conventional stone aggregate by DBC could achieve comparable strength of properly cured moderate strength normal concrete. Application of distorted brick aggregates as internal curing agent or partial replacement of stone chips can save significant amount of money. In addition, environmental problems associated with the dumping of waste bricks in soil can be avoided. The cost of per cubic meter of concrete can also be reduced by 20% partial replacement of stone aggregate. Moreover, such partial replacement will lessen the usage of conventional stone chips and consequently will result in reduction of the depletion of natural resources.

## Appendix A

### List of abbreviations

| | |
|---|---|
| IC | Internal curing/internally cured |
| BC | Brick chips |
| NC | Concrete sample with stone aggregate exposed to adverse curing condition |
| DBC | Distorted brick chips |
| DOE | Department of Environment |
| FCK | Fixed-chimney kiln |
| HHK | Hybrid Hoffman |
| VSBK | Vertical shaft brick kiln |
| RC | Reinforced concrete |
| BUET | Bangladesh University of Engineering and Technology |
| BC | Brick chips |
| SC | Stone chips |
| RH | Relative humidity |
| SEM | Scanning electron microscope |
| TCI | Time to corrosion initiation |
| FIB | International Federation for Structural Concrete |
| CA | Coarse aggregates |
| FA | Fine aggregates |
| OPC | Ordinary Portland cement |
| FM | Fineness modulus |
| OD | Oven dry |
| w/c | Water-to-cement ratio |
| IC(B) | Concrete sample with 20% replacement of SC by BC (Type B) exposed to adverse curing condition |
| IC(E) | Concrete sample with 20% replacement of SC by BC (Type E) exposed to adverse curing condition |
| NCS | Concrete sample with stone aggregate kept under water for 28 days |
| SSD | Saturated surface dry |
| ICB0W | Concrete sample with 20% replacement of SC by BC (Type B) exposed just after casting without any cover |
| ICE0W | Concrete sample with 20% replacement of SC By BC (Type E) exposed just after casting without any cover |
| NC0W | Concrete sample with stone aggregate exposed just after casting without any cover |
| ICB0P | Concrete sample with 20% replacement of SC by BC (Type B) exposed just after casting and covered with polythene |
| ICE0P | Concrete sample with 20% replacement of SC by BC (Type E) exposed just after casting and covered with polythene |
| NC0P | Concrete sample with stone aggregate exposed just after casting and covered with polythene |
| ICB3W | Concrete sample with 20% replacement of SC by BC (Type B) exposed after 3 days of curing under water and without any cover |
| ICE3W | Concrete sample with 20% replacement of SC by BC (Type E) exposed after 3 days of curing under water and without any cover |
| NC3W | Concrete sample with stone aggregate exposed after 3 days of curing under water and covered with polythene |
| ICB3P | Concrete sample with 20% replacement of SC by BC (Type B) exposed after 3 days of curing under water and covered with Polythene |
| ICE3P | Concrete sample with 20% replacement of SC by BC (Type E) exposed after 3 days of curing under water and covered with polythene |

| | |
|---|---|
| NC3P | Concrete sample with stone aggregate exposed after 3 days of curing under water and covered with polythene |
| ICB7W | Concrete sample with 20% replacement of SC by BC (Type B) exposed after 7 days of curing under water and without any cover |
| ICE7W | Concrete sample with 20% replacement of SC by BC (Type E) exposed after 7 days of curing under water and without any cover |
| NC7W | Concrete sample with stone aggregate exposed after 7 days of curing under water and covered with polythene |
| ICB7P | Concrete sample with 20% replacement of SC by BC (Type B) exposed after 7 days of curing under water and covered with polythene |
| ICE7P | Concrete sample with 20% replacement of SC by BC (Type E) exposed after 7 days of curing under water and covered with polythene |
| NC7P | Concrete sample with stone aggregate exposed after 7 days of curing under water and covered with polythene |
| FE-SEM | Field emission scanning electron microscopy |
| RMT | Non-steady-state migration test |
| $D_{nssm}$ | Chloride diffusion co-efficient |
| SR | Surface resistivity |
| $K$ | Geometry factor |
| $R$ | Resipod reading |
| $r$ | Resistivity measured at temperature $T$ |
| $s$ | Spacing of probe |
| $d$ | Diameter of cylindrical specimen |
| $L$ | Length of cylindrical specimen |
| $r_{Tref}$ | Corrected resistivity |
| $E_{a\text{-}cond}$ | Activation energy |
| $R$ | Universal gas constant |
| $T_{ref}$ | Reference temperature (23 °C) |
| EN | European standard |
| XD | Corrosion induced by chlorides other than from sea water |
| XS | Corrosion induced by chlorides from sea water |
| XD1 | Concrete surfaces exposed to airborne chlorides |
| XD2 | Parts of bridges exposed to spray containing chlorides, pavements, car park slabs |
| XS1 | Structure near to or on the coast exposed to airborne salt |
| XS2 | Part of marine structures with the tidal, the splash and spray zone |
| $C_{crit}$ | Critical chloride content |
| $C_0$ | Initial chloride content of the concrete |
| $C_{S,}\Delta x$ | Chloride content at a depth $\Delta x$ and a certain point of time $t$ |
| $\Delta x$ | Depth of the convection zone |
| $D_{crm(to)}$ | Apparent coefficient of chloride diffusion through concrete |
| $k_t$ | Transfer parameter |
| $a$ | Ageing exponent |
| $t_0$ | Reference point of time |
| $b_e$ | Regression variable |
| $T_{ref}$ | Reference temperature |
| $T_{real}$ | Temperature of structural element or ambient air |

**Acknowledgements** The authors would like to pay their sincere gratitude to Brigadier General Md. Wahidul Islam, Former Head, Department of Civil Engineering, Military Institute of Science and Technology (MIST), Dhaka, for his generous support during the study. The authors also acknowledge the assistance of the staff of the Concrete Laboratory of the same Department in carrying out the research work. The authors are also grateful to Dr. M. Hasanuzzaman, Associate Professor, Department of Glass and Ceramic Engineering (GCE), Bangladesh University of Engineering and Technology (BUET), Mr. Shahjalal Rana, Senior Lab Instructor, GCE, BUET and Ms. Sumaiya Afroz, Assistant Professor, Department of Civil Engineering, BUET for SEM images and analysis of images.

**Funding** Not applicable.

## Declarations

**Conflict of interest** The authors of the manuscript titled "Potential of Waste Distorted Bricks to Produce Internally Cured Concrete under Adverse Curing Conditions" declare no conflict of interest of any of the authors with any organization in the subject matter discussed in the manuscript.

**Ethical approval** The study was performed following the accepted ethical standard of a genuine research.

**Informed consent** All the researchers particpated in the study volunatarily and gave their full consent in publishing this article.

## References

1. Masum ATM, Manzur T (2019) Delaying time to corrosion initiation in concrete using brick aggregate as internal curing medium under adverse curing conditions. Constr Build Mater 228:116772
2. Mazumder AR, Kabir A, Yazdani N (2006) Performance of over burnt distorted bricks as aggregates in pavement works. J Mater Civ Eng 18(6):777–785

3. Frankfurt School of Finance and Management (2019) Bangladesh brick sector roadmap 2019–2030. Frankfurt am Main, Germany. https://www.ccacoalition.org/en/resources/bangladesh-brick-sector-road-map. Accessed 12 Mar 2020
4. The World Bank (2011) Introducing energy-efficient clean technologies in the brick sector of Bangladesh. The World Bank, Washington DC. http://siteresources.worldbank.org/BANGLADESHEXTN/Images/295758-1298666789983/7759876-1323201118313/BDBrickFINAL.pdf. Accessed 30 Nov 2019
5. Department of Environment (2017) National strategy for sustainable brick production in Bangladesh. Ministry of Environment and Forests, Government of the People's Republic of Bangladesh
6. Iffat S, Manzur T, Rahman S, Noor MA, Yazdani N (2017) Optimum proportion of masonry chip aggregate for internally cured concrete. Int J Concr Struct Mater 11(3):513–524
7. Iffat S, Manzur T, Noor MA (2017) Durability performance of internally cured concrete using locally available low cost LWA. KSCE J Civ Eng 21(4):1256–1263
8. Bentz DP, Lura P, Roberts JW (2005) Mixture proportioning for internal curing. Concr Int 27(02):35–40
9. Baten B, Manzur T (2020) Masonry chips aggregate as internal curing medium: a cost effective alternative to counteract improper curing conditions. Mater Today Proc 32:594–599
10. Manzur T, Rahman S, Torsha T, Noor MA, Hossain KMA (2019) Burnt clay brick aggregate for internal curing of concrete under adverse curing conditions. KSCE J Civ Eng 23(12):5143–5153
11. Bosunia SZ, Chowdhury JR (2001) Durability of concrete in coastal areas of Bangladesh. J Civ Eng (IEB) 29(1):41–53
12. Manzur T, Iffat S, Noor MA (2015) Efficiency of sodium polyacrylate to improve durability of concrete under adverse curing condition. Adv Mater Sci Eng 2015:685785. https://doi.org/10.1155/2015/685785
13. Afroz S, Rahman F, Iffat S, Manzur T (2015) Sorptivity and strength characteristics of commonly used concrete mixes of Bangladesh. In: International conference on recent innovation in civil engineering for sustainable development (IICSD), Gazipur, Bangladesh
14. Manzur T (2017) Adversecuring conditions and performance of concrete: Bangladesh perspective. Int J Civ Environ Struct Constr Archit Eng 11(4):567–571
15. Manzur T, Mahmood MH, Baten B, Hasan MJ, Hossain MR, Noor MA, Yazdani N (2020) Assessment of progressive collapse proneness of existing typical garment factory buildings in Bangladesh. J Perform Constr Facil 34(5):04020092
16. Manzur T, Hasan MJ, Baten B, Torsha T, Khan MFA, Hossain KMA (2019) Significance of service life based concrete mix design in marine environment. In: 7th International conference on engineering mechanics & materials by CSCE, Laval Greater Montreal, Canada
17. ASTM C39 (2014) Standard test method for compressive strength of cylindrical concrete specimens. American Society for Testing and Materials
18. NT BUILD 492 (1999) Concrete, mortar and cement based repair materials: chloride migration coefficient from non-steady state migration experiments. NORDTEST, Finland
19. FIB Bulletin 34 (2006) Model code for service life design, international federation for structural concrete
20. Lizarazo-Marriaga J, Claisse P (2009) Determination of the concrete chloride diffusion coefficient based on an electrochemical test and an optimization model. Mater Chem Phys 117(2–3):536–543
21. Yang CC, Wang LC (2004) The diffusion characteristic of concrete with mineral admixtures between salt ponding test and accelerated chloride migration test. Mater Chem Phys 85(2–3):266–272
22. Baten B, Manzur T, Ahmed I (2020) Combined effect of binder type and target mix-design parameters in delaying corrosion initiation time of concrete. Constr Build Mater 242:118003
23. Baten B, Manzur T, Torsha T, Alam S (2021) A parametric study on the graphical approach to assess corrosion vulnerability of concrete mixes in chloride environment. Constr Build Mater 309:125115
24. Kim YY, Lee KM, Bang JW, Kwon SJ (2014) Effect of w/c ratio on durability and porosity in cement mortar with constant cement amount. Adv Mater Sci Eng 2014:273460. https://doi.org/10.1155/2014/273460
25. Mahima S, Moorthi PVP, Bahurudeen A, Gopinath A (2018) Influence of chloride threshold value in service life prediction of reinforced concrete structures. Sādhanā 43(7):115
26. Alonso C, Andrade C, Castellote M, Castro P (2000) Chloride threshold values to depassivate reinforcing bars embedded in a standardized OPC mortar. Cem Concr Res 30(7):1047–1055
27. Ahmad S (2003) Reinforcement corrosion in concrete structures, its monitoring and service life prediction—a review. Cem Concr Compos 25:459–471
28. Wang X, Nguyen M, Stewart MG, Syme M, Leitch A (2010) Analysis of climate change impacts on the deterioration of concrete infrastructure—part 1: mechanisms, practices, modelling and simulations—a review. CSIRO, Canberra, p 8 (**ISBN, 9780(4310365)**)
29. Zhou Y, Gencturk B, Willam K, Attar A (2014) Carbonation-induced and chloride-induced corrosion in reinforced concrete structures. J Mater Civ Eng 27(9):04014245
30. Khan MU, Ahmad S, Al-Gahtani HJ (2017) Chloride-induced corrosion of steel in concrete: an overview on chloride diffusion and prediction of corrosion initiation time. Int J Corros 2017:5819202. https://doi.org/10.1155/2017/5819202
31. Manzur T, Baten B, Hasan MJ, Akter H, Tahsin A, Hossain KMA (2018) Corrosion behavior of concrete mixes with masonry chips as coarse aggregate. Constr Build Mater 185:20–29
32. ASTM C136 (2006) Standard test method for sieve analysis of fine and coarse aggregates. American Society for Testing and Materials
33. ASTM C127 (2012) Standard test method for density, relative density (specific gravity), and absorption of coarse aggregate. American Society for Testing and Materials
34. ASTM C128 (2012) Standard test method for density, relative density (specific gravity), and absorption of fine aggregate. American Society for Testing and Materials
35. ASTM C29 (2009) Standard test method for bulk density ("unit weight") and voids in aggregate. American Society for Testing and Materials
36. ASTM C187 (2011) Standard test method for normal consistency of hydraulic cement. American Society for Testing and Materials
37. ASTM C191 (2013) Standard test methods for time of setting of hydraulic cement by Vicat Needle. American Society for Testing and Materials
38. ASTM C204 (2011) Standard test method for fineness of hydraulic cement by air-permeability apparatus. American Society for Testing and Materials
39. ASTM C109 (2013) Standard test method for compressive strength of hydraulic cement mortars (Using 2-in. or [50-mm] Cube Specimens). American Society for Testing and Materials
40. ASTM C150 (2012) Standard specification for Portland cement. American Society for Testing and Materials
41. ASTM C1761 (2012) Standard specification for lightweight aggregate for internal curing of concrete. American Society for Testing and Materials
42. EN, B.S, 206-1 (2000) Concrete-part 1: specification, performance, production and conformity. British Standards Institution

43. AASHTO TP 95 (2014) Method of test for surface resistivity indication of concrete's ability to resist chloride ion penetration. American Association of State Highway and Transportation Officials
44. Baten B, Manzur T (2022) Formation factor concept for non-destructive evaluation of concrete's chloride diffusion coefficients. Cem Concr Compos 128:104440
45. Spragg RP, Bu Y, Snyder KA, Bentz DP, Weiss J (2013) Electrical testing of cement based materials: role of testing techniques, sample conditioning, and accelerated curing. Joint Transportation Research Program, Indiana Department of Transportation, and Purdue University, Report No. FHWA/IN/JTRP-2013/28
46. Spragg R, Villani C, Snyder K, Bentz D, Bullard J, Weiss J (2013) Factors that influence electrical resistivity measurements in cementitious systems. Transp Res Rec 2342:90–98
47. Spragg RP (2017) Development of performance related specifications that include formation factor. Ph.D. dissertation, Purdue University
48. Gowers KR, Millard SG (1999) Measurement of concrete resistivity for assessment of corrosion severity of steel using Wenner technique. ACI Mater J 96(5):536–541
49. Morris W, Moreno E, Sagues A (1996) Practical evaluation of resistivity of concrete in test cylinders using a Wenner array probe. Cem Concr Res 26(12):1779–1787
50. DuraCrete (1998) Modelling of degradation, duracrete—probabilistic performance based durability design of concrete structures. EU - Brite EuRam III, Contract BRPR-CT95-0132, Project BE95-1347/R4-5
51. DARTS (2004) Durable and reliable tunnel structures: deterioration modelling. European commission. Growths 2000, Contract G1RD-CT-2000-00467, Project GrD1-25633
52. Afroz S, Manzur T, Hossain KMA (2020) Arrowroot as bio-admixture for performance enhancement of concrete. J Build Eng 30:101313
53. Cultrone G, Sebastian E, Elert K, De la Torre MJ, Cazalla O, Rodriguez-Navarro C (2004) Influence of mineralogy and firing temperature on the porosity of bricks. J Eur Ceram Soc 24(3):547–564
54. Baiden BK, Agyekum K, Ofori-Kuragu JK (2014) Perceptions on barriers to the use of burnt clay bricks for housing construction. J Constr Eng 2014:502961.https://doi.org/10.1155/2014/502961
55. Public Works Department (2019) Standard schedule of rates for civil works. Government of the People's Republic of Bangladesh